

Synthesis and Characterization of Organic Photo-Sensitizers Containing Multi-Acceptors for the Application of Dye-Sensitized Solar Cells

HYO JEONG JO,¹ YOUNG CHEOL CHOI,²
JANG-HYUN RYU,³ JUNG HYEON KANG,³
NAM KYU PARK,³ DO KYUNG LEE,²
AND JAE HONG KIM¹

¹Department of Display and Chemical Engineering, Yeungnam University, Gyeongsan, Gyeongsangbuk-do, Republic of Korea

²R&D Affairs Department, Gumi Electronics & Information Technology Research Institute, Gumi, Gyeongsangbuk-do, Republic of Korea

³Solar Cell Research Center, Korea Institute of Science and Technology (KIST), Seoul, Republic of Korea

Organic photo-sensitizers containing multi-acceptors in a chromophore have been synthesized and characterized for the application of dye-sensitized solar cell (DSSC). In this study, we have used intramolecular push-pull system containing triphenylamine as the electron donor with different number of cyanoacetic acid moieties as electron acceptor/anchoring groups in a chromophore. The experimental results have revealed that when the induced electron acceptor increases, the larger amounts of dyes are adsorbed on the TiO₂ surface in DSSC, resulting in the increase of short circuit photocurrent density. Our results suggest that the organic dyes with multi-electron acceptors moieties are promising for getting higher solar-to-electricity conversion efficiencies in DSSC.

Keywords Dye-sensitized solar cells; intramolecular charge-transfer chromophore; multi-acceptors; organic photo-sensitizers

1. Introduction

Since Grätzel *et al.* reported the first efficient dye-sensitized solar cells (DSSCs) in 1991 [1], they have attracted much attention due to their relatively high power conversion efficiency and potentially low cost production [2–10]. To date, high performance and good stability of DSSC based on Ru-dyes as a photosensitizer had

Address correspondence to Prof. Jae Hong Kim, School of Display and Chemical Engineering, Yeungnam University, 214-1 Dae-dong, Gyeongsan, Gyeongsangbuk-do 712-749, Korea (ROK). Tel.: (+82)53-810-2521; Fax: (+82)53-810-4631; E-mail: Jaehkim@ynu.ac.kr or Dr. Do Kyung Lee, R&D Affairs Department, Gumi Electronics & Information Technology Research Institute, Bongsan-ri, Sandong-Myeon, Gumi, Gyeongsangbuk-do 730-853, Korea (ROK). Tel.: (+82)54-479-2111; Fax: (+82)54-479-2050; E-mail: dklee@geri.re.kr

been widely addressed in the literatures. The DSSC with Ru-bipyridyl complexes (N3 and N719), and the one with black ruthenium dye have achieved power conversion efficiencies up to 11.2% and 10.4%, respectively [3,4].

However, the Ru-based dyes are facing the problem of manufacturing costs and environmental issues. In order to obtain the cheaper photosensitizers for the DSSC, the metal-free organic photosensitizers are strongly desired. The metal-free organic dyes offer superior molar extinction coefficients, low cost, and diverse molecular structures as compared to the conventional Ru-based dyes. Recently, novel photosensitizers such as coumarin [5], merocyanine [6], cyanine [7], indoline [8], hemicyanine [9], triphenylamine [10–13], dialkylaniline [14], bis(dimethylfluorenyl)-aminophenyl [15,16], phenothiazine [17], tetrahydroquinoline [18], and carbazole [19] based dyes have achieved the solar-to-electrical power conversion efficiencies up to 5–9%.

In general, organic dyes are designed to be of intramolecular donor-acceptor structure that is called a push-pull architecture, which can induce the electron density change from electron donor to electron acceptor by the light irradiation following subsequent electron injection to the TiO_2 via the anchoring group.

Recently, we have reported [20] the organic dyes with double electron acceptors in a chromophore as a photosensitizer. It was indicated that the organic dyes with double electron acceptors exhibited the high power conversion efficiency in the DSSC due to the increase of electron extraction paths from electron donor as compared with those of single electron acceptor type. Also, this earlier report has the important implications for the needs of conducting studies on the organic dyes containing multi-acceptors with a viewpoint of photovoltaic performance.

In this work, we have studied on the synthesis and characterization of the organic dyes containing different number of electron acceptor moieties in a molecule. In particular, photovoltaic properties of the dyes in DSSC device are mainly discussed.

2. Experimental

2.1. Synthesis

Organic dyes based triphenylamine were synthesized by the well-known reactions such as Vilsmeier-Haack formulation reaction and Knoevenagel reaction. 4-(Diphenylamino)-benzaldehyde, 4,4'-(phenylazanediyl) dibenzaldehyde and 4,4', 4''-(phenyl azanediyl)tribenzaldehyde were prepared by treating triphenylamine with different equivalent of POCl_3 in DMF, according to the procedures in literature [21]. The detailed synthetic procedures for the organic dyes were described as follows.

4-Formyltriphenylamine (1a). Triphenylamine (40 g, 163 mmol) was dissolved in 80 mL DMF. POCl_3 (76 mL, 815 mmol) was added drop to drop to the mixture at 0°C . As the temperature was increased to room temperature, the mixture was changed to a clear bright red solution. The reaction mixture was heated to 45°C and then stirred for an additional 2 hr. The mixture was poured in an ice-bath and then neutralized with sodium bicarbonate. Recrystallization of resulting precipitates from ethanol afforded crystals of 4-Formyltriphenylamine. Pale yellow solids were collected by filtering. (42.9 g, 96%). ^1H NMR (300 MHz, CDCl_3): δ 9.79 (s, 1H), 7.30–7.36 (t, 4H), 7.67 (d, 2H), 7.15–7.18 (m, 6H), 7.00 (d, 2H).

4'4''-Diformyltriphenylamine (1b). Triphenylamine (4.900 g, 20 mmol) and anhydrous DMF (40 mL) were added to a 250-mL round bottomed flask under

nitrogen. The mixture was cooled to 0°C and phosphorus oxychloride (18.0 mL, 200 mmol) was added drop to drop. The mixture was heated to 85°C for 10 hr and the ensuing mixture was poured into an ice water. The mixture was neutralized to pH 7 with aqueous 2 N NaOH solution and then the crude product was extracted with dichloromethane. The product was purified by column chromatography (silicagel, petroleum ether/ethyl acetate=4:1) to obtain pure product (4.81 g, 80%). ¹H NMR (300 MHz, CDCl₃): δ 9.89 (s, 2H), 7.76–7.78 (d, 4H), 7.38–7.41 (t, 2H), 7.25–7.28 (t, 1H), 7.17–7.19 (m, 6H).

4,4',4''-(Phenyl azanediyl)tribenzaldehyde (1c). Triphenylamine (4.900 g, 20 mmol) and anhydrous DMF (40 mL) were added to a 250-mL round bottomed flask under nitrogen. The mixture was cooled to 0°C and phosphorus oxychloride (18.0 mL, 300 mmol) was added drop by drop. The reacting mixture was stirred at 85°C for 10 hr and the ensuing mixture was poured into ice water. It was neutralized to pH 7 with aqueous 2 N NaOH solution, and the crude product extracted with dichloromethane. The product was collected by filtration and purified by column chromatography (silicagel, petroleum ether/ethyl acetate=4:1) to obtain pure product (1.97 g, 30%). ¹H NMR (300 MHz, DMSO-*d*₆): δ 9.85 (s, 3H), 7.83–7.781 (d, 6H), 7.20–7.17 (d, 6H).

2-Cyano-3-(4-diphenylamino-phenyl)-acrylic Acid (TPA1). 4-(Diphenylamino) benzaldehyde (1 g, 3.7 mmol) and 2-cyanoacetic acid (0.47 g, 5.5 mmol) were added to 15 mL of glacial acetic acid and refluxed for 3 hr in the presence of 0.42 g (5.5 mmol) of ammonium acetate. After cooling to room temperature, the mixture was poured into ice water. The precipitate was filtered, washed by distilled water, dried under vacuum, and purified by column chromatography (ethyl acetate/ethanol=9:1), resulting in yellow powder of TPA1 (0.23 g, 80%). ¹H NMR (300 MHz, DMSO-*d*₆): δ 8.13 (s, 1H), 7.90–7.93 (d, 2H), 7.40–7.43 (t, 4H), 7.20–7.27 (m, 6H), 6.84–6.87 (d, 2H).

2-Cyano-3-(4-(phenyl(4-vinylphenyl)amino)phenyl)acrylic Acid (TPA2). 4,4'-(phenylazanediyl)dibenzaldehyde (0.5 g, 1.7 mmol) and 2-cyanoacetic acid (0.31 g, 3.7 mmol) were added to 15 mL of glacial acetic acid and refluxed for 3 hr in the presence of 0.28 g (3.7 mmol) of ammonium acetate. After cooling to room temperature, the mixture was poured into ice water. The precipitate was filtered and washed by distilled water. The product was purified by column chromatography (ethyl acetate/ethanol=8:2), resulting in orange powder of TPA2 (305 mg, 65%). ¹H NMR (300 MHz, DMSO-*d*₆): δ 8.23 (s, 2H), 8.01–8.04 (d, 4H), 7.47–7.51 (t, 2H), 7.32–7.36 (t, 1H), 7.23–7.26 (d, 2H), 7.16–7.18 (d, 4H).

3-(4-{[4-(2-Carboxy-2-cyano-vinyl)-phenyl]-phenyl-amino}-phenyl)-2-cyano-acrylic Acid (TPA3). 4,4',4''-(phenylazanediyl)tribenzaldehyde (0.3 g, 0.3 mmol) and 2-cyanoacetic acid (0.09 g, 1.0 mmol) were added to 15 mL of glacial acetic acid and refluxed for 3 hr in the presence of 0.08 g (1 mmol) of ammonium acetate. After cooling to room temperature, the mixture was poured into ice water. The precipitate was filtered and washed by distilled water. The product was purified by column chromatography (Ethyl acetate/ethanol=7:3), resulting in dark orange powder of TPA3 (0.4 g, 85%). ¹H NMR (300 MHz, DMSO-*d*₆): δ 7.91 (s, 3H), 7.77–7.80 (d, 6H), 7.01–7.04 (d, 6H).

2.2. Fabrication Method of Dye-Sensitized Solar Cell (DSSC)

The fabrication procedure of DSSC is as follows. The conducting glass substrate (FTO; TEC8, Pilkington, $8\ \Omega/\text{cm}^2$, Thickness of 2.3 mm) was cleaned in ethanol by ultrasonication. TiO_2 pastes were prepared using ethyl cellulose (Aldrich), Lauric acid (Fluka) and Terpineol (Aldrich). The size of TiO_2 particles is ca. 20–30 nm. The prepared TiO_2 paste was coated on the pre-cleaned conducting glass substrate using doctor-blade, and sintered at 500°C for 30 min. The thickness of the sintered TiO_2 layer was measured with Alpha-step IQ surface profiler (KLA Tencor). The TiO_2 paste as scattering layer was re-coated over the sintered layer using ca. 250 nm size of TiO_2 particle and then sintered again at 500°C for 30 min. The prepared TiO_2 film was dipped in 0.04 M of TiCl_4 aqueous solution at 70°C for 30 min. For dye adsorption, the annealed TiO_2 electrodes were immersed in dye solution (0.5 mM of dye in DMF; TPA series or N3/N719) at 50°C for 3 hr. Pt counter electrodes were prepared by thermal reduction of thin film formed from 7 mM of H_2PtCl_6 in 2-propanol at 400°C for 20 min. The dye-adsorbed TiO_2 electrode and Pt counter electrode were assembled using 60 μm -thick Surlyn (Dupont 1702) as a bonding agent. A liquid electrolyte was introduced through a pre-punctured hole on the counter electrode. The electrolyte was composed of 3-propyl-1-methyl-imidazolium iodide (PMII, 0.7 M), lithium iodide (LiI, 0.2 M), iodine (I_2 , 0.05 M), and *t*-butylpyridine (TBP, 0.5 M) in acetonitrile/valeronitrile (85:15). The active areas of the dye-adsorbed TiO_2 films were estimated by a digital microscope camera with an image-analysis-software (Moticam 1000).

2.3. Instrumental Analysis

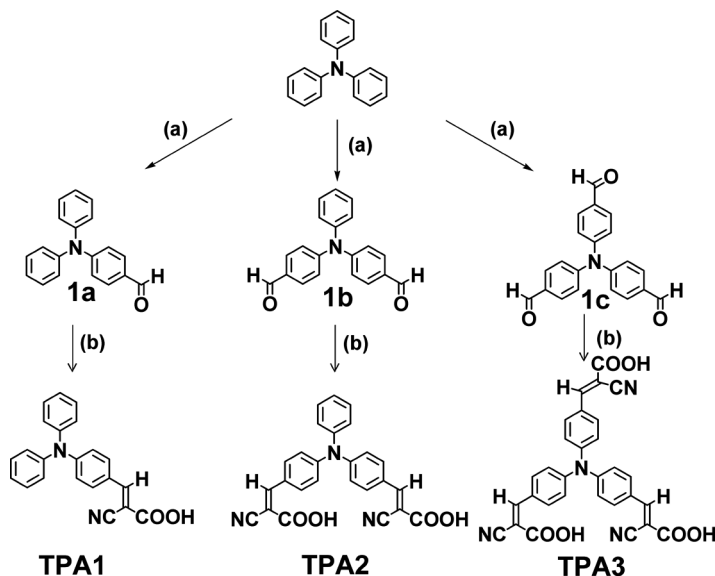
^1H NMR spectra were recorded on a Varian Mercury NMR 300 Hz spectrometer. The redox properties of three dyes were examined using a cyclic voltammetry (Model:CV-BAS-Epsilon) with 100 mV/s scan rate. The electrolyte solution was 0.10 M tetrabutylammonium hexafluorophosphate (TBAPF_6) in freshly dried acetonitrile. The Ag/AgCl and Pt wire (0.5 mm in diameter) electrodes were utilized as reference and counter electrodes, respectively.

3. Results and Discussion

3.1. Synthesis and Optical Properties of Organic Dyes

The intramolecular electron donor-acceptor type of organic dyes, which are containing triphenylamine as an electron donor and cyanoacetic acid as an acceptor, were synthesized as shown in Scheme 1. The organic photosensitizers containing multi-electron acceptor/anchoring groups, TPA2 and TPA3, were synthesized to investigate the correlation between the number of acceptors and photon-to-current efficiency.

Figure 1 shows the UV-Vis absorption spectra of the synthesized dyes in DMSO solution (a) and on the TiO_2 film (b). It is observed that the molar extinction coefficient of the dye increases with increasing the number of electron acceptor in a chromophore. The absorption peaks of the organic dyes adsorbed on the TiO_2 surface are found to be slightly blue-shifted, compared with those of solution state. This blue-shift of absorption peak may be caused by the formation of the H-aggregate of organic dyes on the TiO_2 surface. The optical and electrochemical properties of the organic dyes are summarized in Table 1.



Scheme 1. Synthetic procedures and molecular Structures of organic dyes (a) DMF, POCl₃, 1,2-dichloroethane, and (b) cyanoacetic acid, NH₄OAc, CH₃COOH.

3.2. Electrochemical Properties

Highly efficient DSSC requires that the LUMO level of dye molecules should be more negative than the conduction band edge of TiO₂ to ensure the effective electron injection from the excited dye molecules to the conduction band of TiO₂ film and that the HOMO level of the dye should be more positive than the redox potential of I₃⁻/I⁻ to ensure the regeneration of dye molecules [22]. The HOMO levels of the dye molecules have been estimated from the cyclic voltammetry curves, as shown in Figure 2. The HOMO levels of TPA2 and TPA3 containing multi-acceptors in a chromophore show similar energy level with -5.57 and -5.54 eV, respectively. Those

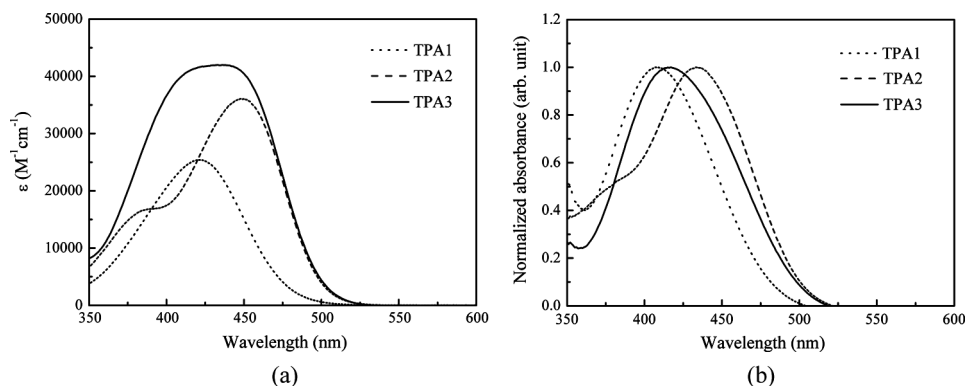


Figure 1. (a) Absorption spectra of TPA1, TPA2, and TPA3 dyes dissolved in DMSO, and (b) absorption spectra of the as-synthesized dyes absorbed on TiO₂ films, which were measured in the diffuse reflectance mode.

Table 1. Optical and electrochemical properties of organic dyes

Dye	$\epsilon_{\text{max}}^a / \text{M}^{-1} \text{cm}^{-1}$	$\lambda_{\text{max}}^a / \text{nm}$ Soln. TiO_2	$\lambda_{\text{em}}^b / \text{nm}$	$E_{0-0}^c (\text{eV})^c$ (abs/em)	E_{ox}^d (V vs NHE)	$E_{\text{ox}}-E_{0-0}^d$ (V vs NHE)	HOMO (eV)	LUMO (eV)
TPA1	25413	421 407	518	2.69	0.93	-1.76	-5.38	-2.69
TPA2	36099	448 433	514	2.35	1.09	-1.26	-5.57	-3.22
TPA3	41980	433 415	514	2.46	1.06	-1.40	-5.54	-3.08

^{a,b} Absorption and emission spectra were measured in DMSO solution. The emission spectra were obtained with the concentration of $5 \times 10^{-5} \text{ M}$ at 293 K. ϵ_{max} is the molar extinction coefficient at λ_{max} of absorption.

^cThe zeroth-zeroth transition E_{0-0} values were estimated from the intersection of the absorption spectra.

^dCyclic voltammetry of the oxidation behavior of the dyes was measured in dry acetonitrile containing 0.1 M tetrabutylammonium hexafluorophosphate (TBAPF₆) as supporting electrolyte (working electrode, glassy carbon; reference electrode, Ag/Ag⁺ calibrated with ferrocene/ferrocenium (Fc/Fc⁺) as an internal reference; counter electrode, Pt). HOMO(eV) = -4.8-($E_{\text{onset}}-E_{\text{Ferrocene}}$).

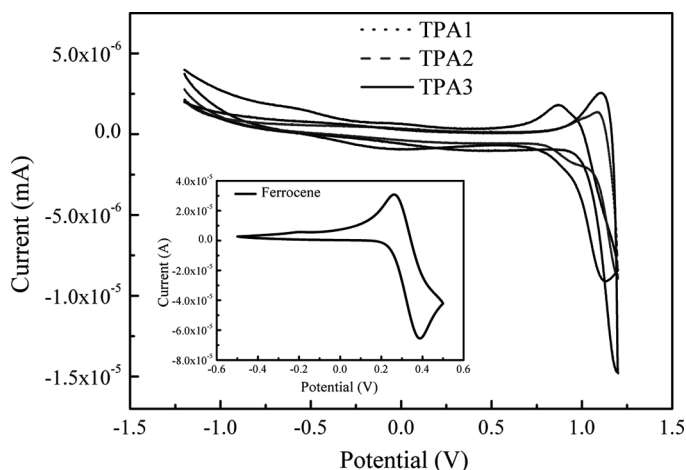


Figure 2. Cyclic voltammograms of the organic dyes.

values are more negative to compare with that of single acceptor system in TPA1. The zeroth-zeroth transition E_{0-0} values have been estimated from the cross-point of the normalized UV absorption spectra; the LUMO levels of the dyes have been calculated from the following equation: $E_{\text{LUMO}} = E_{\text{HOMO}} - E_{0-0}$; and the results are also summarized in Table 1.

3.3. Photovoltaic Performance of the Dyes

The photovoltaic performance of organic dyes and the amount of dyes adsorbed on the surface of TiO_2 in DSSC are summarized in Table 2. For comparison, the efficiency of DSSC device with N719 dye under the same conditions is also indicated in Table 2, which is represented the power conversion efficiency of 8.3%. The corresponding photocurrent-voltage curves are shown in Figure 3. The organic dyes containing multi-acceptor, TPA2 and TPA3, show better photovoltaic properties in a short circuit photocurrent density (J_{sc}) of 8.7 and 8.0 mAcm^{-2} , compared with that of TPA1 in 7.1 mAcm^{-2} . The more dye adsorbed on the TiO_2 surface, the better J_{sc} is observed. In the case of TPA3 with three acceptor moieties in a chromophore, it shows relatively low open circuit voltage (V_{oc}) to compare with that of TPA2 in

Table 2. DSSC performance data of organic dyes^a

Dye	J_{sc}/mAcm^{-2}	V_{oc}/mV	FF/%	$\eta/\%$	Active area/ cm^2	Layer thicken./ μm	Amount/ $10^{-8} \text{ mol cm}^{-2}$
TPA1	7.1	732.7	70.62	3.7	0.421	7.46	223
TPA2	8.7	740.3	69.95	4.5	0.433	7.35	815
TPA3	8.0	630.0	65.73	3.3	0.393	7.41	554
N719	15.6	780.0	68.45	8.3	0.464	6.20	2099

^aWith scattering layer (250 nm, 4 μm) + TiCl_4 Treatment on FTO glass, Blocking layer, TiO_2 paste : B32, Organic Dye 0.5 mM, PMH (0.7 M) + LiI (0.2 M) + I_2 (0.05 M) + TBP (0.5 M) in ACN/VN = 85:15, Pt electrode solution (7 mM), 60 μm surlyn, Dr.blade (2 T).

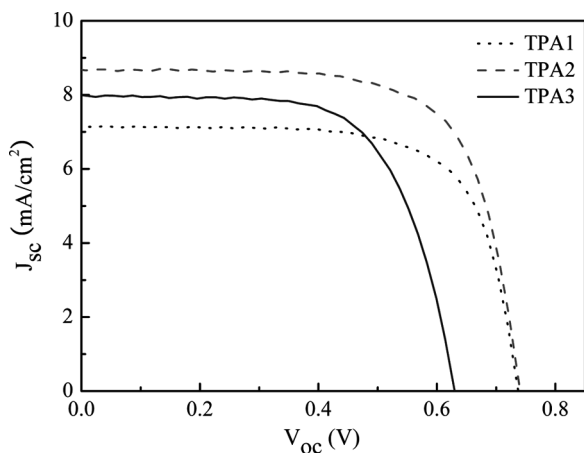


Figure 3. Photocurrent density versus voltage curves of the organic dyes for DSSC.

the DSSC, which affects the efficiency of DSSC, significantly. It has been reported that for photo-sensitizers containing protonated carboxylic groups, anchoring groups are adsorbed the TiO₂ surface and hence most of their protons transfer to the TiO₂ [3]. Therefore, the multi-anchoring TPA3 can supply a higher concentration of the proton onto the TiO₂ surface than that of the single-anchoring TPA1. The high proton concentration gives rise to the larger positive charges on the TiO₂ surface, leading to the increasing recombination rate and the lowering V_{oc} value in DSSC. This is because that the increase in the recombination reaction contribute to the decrease of the energy gap between the redox couple of iodine/tri-iodide and the Fermi level, resulting from the lowering the Fermi level of TiO₂. The electron recombination dynamic experiment for the multi-anchoring TPA3 is needed for the further information.

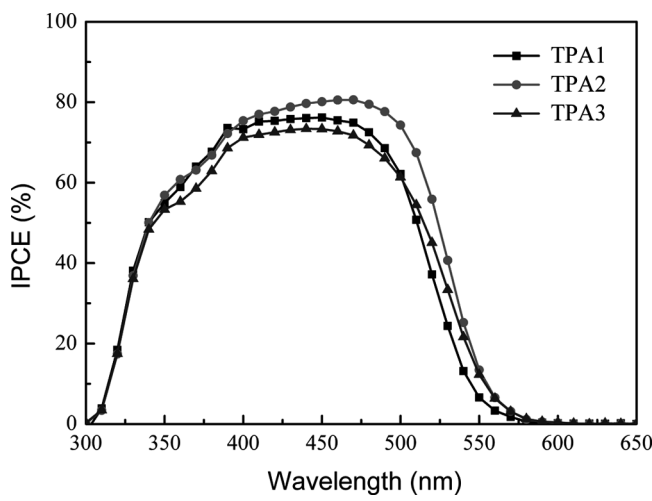


Figure 4. Spectra of monochromatic incident photon-to-current conversion efficiencies for DSSC based on the organic dyes.

The incident photon-to-current conversion efficiencies (IPCEs) for the DSSCs have been also detected with light from a 500-W Xe lamp that is focused through a monochromator onto the photovoltaic cell and their results are shown in Figure 4. The IPCE values are determined at 5 nm intervals according to Eq. (1) [23].

$$\text{IPCE \% } (\lambda) = \frac{1240(\text{eV} \cdot \text{nm})}{\lambda(\text{nm})} \times \frac{J_{\text{sc}}(\text{mA}/\text{cm}^2)}{\phi(\text{mW}/\text{cm}^2)} \times 100 \quad (1)$$

The IPCE of organic dyes shows more than 70% in a spectral range from 400 nm to 500 nm. The highest value 83% is detected in TPA2 at 460 nm, which is good agreement with the result of J_{sc} value in Table 2.

4. Conclusions

We have designed and synthesized the organics dyes with multi-electron acceptor moieties in a chromophore. Effects of the number of electron acceptors in a chromophore and their photovoltaic properties in the DSSC device have been also demonstrated in this work. Compared to other dyes, the DSSC based on TPA2 shows the most efficient solar-to-electrical power conversion efficiency, which is the maximum η value of 4.5% ($V_{\text{oc}} = 740$ mV, $J_{\text{sc}} = 8.7$ mA/cm², FF = 0.68%) under simulated AM 1.5 irradiation (100 mW/cm²). Also, the larger amount of protonated carboxylic groups in the multi-anchoring organic dye, TPA 3, led to the increase in the recombination reaction, resulting in the decrease of the open-circuit voltage in DSSC. A study on the electron recombination dynamics of TPA3 and the stability of DSSC based on the organic dyes are now in progress.

Acknowledgments

This work was supported by National Research Foundation of Korea Grant funded by the Korean Government (2009-0067142).

References

- [1] O'Regan, B., & Grätzel, M. (1991). *Nature*, 353, 737.
- [2] Liu, X., Luo, Y., Li, H., Fan, Y., Yu, Z., Lin, Y., Chen, L., & Meng, Q. (2007). *Chem. Commun.*, 9, 2847.
- [3] Nazeeruddin Mohammad, K., Angelis, F. D., Fantacci, S., Selloni, A., Viscardi, G., Liska, P., Ito, S., Takeru, B., & Grätzel, M. (2005). *J. Am. Chem. Soc.*, 127, 16835.
- [4] Nazeeruddin Mohammad, K., Pechy, P., Renouard, T., Zakeeruddin, S. M., Humphry-Baker, R., Comte, P., Liska, P., Cevey, L., Costa, E., Shklover, V., Spiccia, L., Daecon, G. B., Bignozzi, C. A., & Grätzel, M. (2001). *J. Am. Chem. Soc.*, 123, 1613.
- [5] Hara, K., Sato, T., Katoh, R., Furube, A., Ohga, Y., Shinpo, A., Suga, S., Sayama, K., Sugihara, H., & Arakawa, H. (2003). *J. Phys. Chem. B*, 107, 597.
- [6] Sayama, K., Hara, K., Sugihara, H., Arakawa, H., Mori, N., Satsuki, M., Suga, S., Tsukagoshi, S., & Abe, Y. (2000). *Chem. Commun.*, 1173.
- [7] Ehret, A., Stuhl, L., & Spitler, M. T. (2001). *J. Phys. Chem. B*, 105, 9960.
- [8] Horiuchi, T., Miura, H., Sumioka, K., & Uchida, S. (2004). *J. Am. Chem. Soc.*, 126, 12218.

- [9] Wang, Z., Li, F., & Huang, C. (2000). *Chem. Commun.*, 2063.
- [10] Liang, M., Xu, W., Cai, F., Chen, P., Peng, B., Chen, J., & Li, Z. (2007). *J. Phys. Chem. C*, *111*, 4465.
- [11] Velusamy, M., Thomas, K. R. J., Lin, J. T., Hsu, Y., & Ho, K. (2005). *Org. Lett.*, *7*, 1899.
- [12] Tsai, M., Hsu, Y., Lin, J. T., Chen, H., & Hsu, C. (2007). *J. Phys. Chem. C*, *111*, 18785.
- [13] Thomas, K. R. J., Hsu, Y. C., Lin, J. T., Lee, K. M., Ho, K. C., Lai, C. H., Cheng, Y. M., & Chou, P. T. (2008). *Chem. Mater.*, *20*, 1830.
- [14] Hara, K., Sato, T., Katoh, R., Furube, A., Yoshihara, T., Murai, M., Kurashige, M., Ito, S., Shinpo, A., Suga, S., & Arakawa, H. (2005). *Adv. Funct. Mater.*, *15*, 246.
- [15] Kim, S. h., Lee, J. K., Kang, S. O., Ko, J. J., Yum, J. H., Fantacci, S., De Angelis, F., Di Censo, D., Nazeeruddin, Md. K., & Grätzel, M. (2006). *J. Am. Chem. Soc.*, *128*, 16701.
- [16] Choi, H., Lee, J. K., Song, K., Kanga, S. O., & Ko, J. (2007). *Tetrahedron*, *63*, 3115.
- [17] Tian, H., Yang, X., Chen, R., Pan, Y., Li, L., Hagfeldt, A., & Sun, L. (2007). *Chem. Commun.*, 3741.
- [18] Chen, R., Yang, X., Tian, H., & Sun, L. (2007). *J. Photochem. Photobio. A. Chem.*, *189*, 295.
- [19] Koumura, N., Wang, Z., Mori, S., Miyashita, M., Suzuki, E., & Hara, K. (2006). *J. Am. Chem. Soc.*, *128*, 14256.
- [20] Park, S. S., Won, Y. S., Choi, Y. C., & Kim, J. H. (2009). *Energy & Fuels*, *23*, 3732.
- [21] Smestad, G. (1994). *Solar Energy Materials and Solar Cells*, *32*, 273.
- [22] Kuang, D., Ito, S., Wenger, B., Klein, C., Moser, J. E., Humphry, B., Robin, Zakeeruddin, Shaik, M., & Grätzel, M. (2006). *J. Am. Chem. Soc.*, *128*, 4146.
- [23] Wei, X., Bo, P., Jun, C., Mao, L., & Fengshi, C. (2008). *J. Phys. Chem. C*, *112*, 874.